

ANODIC SULFIDATION OF FeS ELECTRODE IN A NaCl SATURATED AlCl_3 -NaCl MELT

NORIO TAKAMI and NOBUYUKI KOURA

(Received 1 December 1987; in revised form 23 February 1988)

Department of Industrial Chemistry, Faculty of Science and Technology, Tokyo University of Science, 2641, Yamazaki, Noda, Chiba 278, Japan

Abstract—Cyclic voltammogram of a FeS electrode in an AlCl_3 -NaCl melt saturated with NaCl containing dissolved Al_2S_3 was found to be similar to that of the positive electrode of an Al/FeS₂ secondary cell. Anodic sulfidation of the FeS in the melt was characterized as the oxidation reaction which produces FeS₂ under diffusion control of a sulfide ion as AlSCl_2^- by using cyclic voltammetry, *ac* impedance measurements, and X-ray analysis. Moreover, from the detailed analysis of the results, the mechanism for the anodic reaction was proposed to be $\text{FeS} + \text{AlSCl}_2^- + 2\text{Cl}^- \rightleftharpoons \text{FeS}_2 + \text{AlCl}_4^- + 2e^-$. The diffusion coefficient of the AlSCl_2^- was calculated to be $1 \times 10^{-6} \text{ cm}^2 \text{ s}^{-1}$ at 240°C.

INTRODUCTION

We have developed an Al/FeS₂ secondary cell with a molten AlCl_3 -NaCl electrolyte for both load-levelling and electric vehicle applications[1-4]. The cell is usually operated at 170-250°C and has a basic AlCl_3 -NaCl melt as an electrolyte. An understanding of the electrochemical characteristics of the FeS₂ electrode is important for the further development of such cells. In previous studies, the cathodic reaction of the FeS₂ electrode has been investigated in order to improve the discharge performance. During the discharge process, the positive electrode was considered to be converted from FeS₂ to FeS and "Al₂S₃". Here, the "Al₂S₃" indicates some kind of species of dissolved aluminum sulfide of which the structure is unknown. It was found that the cathodic reaction consists of the charge transfer, the surface reaction, and the diffusion processes[5]. The charging processes are not clear, however, they appear to affect the cycle life and rechargeability of the cell. In the present paper, we report the preliminary results of studies on the anodic sulfidation reaction of FeS in molten AlCl_3 -NaCl saturated with NaCl containing dissolved Al_2S_3 which corresponds to the charging conditions of the positive electrode in the cell. The anodic behavior was investigated by cyclic voltammetry, *ac* impedance measurements, X-ray analysis, scanning electron microscopy, and EMF measurements.

EXPERIMENTAL

The AlCl_3 -NaCl electrolyte was prepared by heating an anhydrous aluminum chloride (G.R., Pb < 0.01%, Fe < 0.02%, Yotsubata Chemicals) and sodium chloride (G.R. Wako Pure Chemicals) mixture in a dry N₂ filled Pyrex tube at 180°C, that was in contact with Al wire (99.99% purity, 1 mm diam.) for 48 h in order to remove any trace amount of im-

purities. The electrolyte was usually an AlCl_3 -NaCl melt (48 mol% AlCl_3 -52 mol% NaCl) saturated with NaCl. The melts containing Al_2S_3 (Alfa Products) were made by heating at 200°C until the Al_2S_3 was mostly dissolved.

The positive electrode was a paste electrode (5 cm² × 0.7 cm) composed of a synthesized FeS₂ powder (2.5 g, Asahikasei), a graphite powder (1.0 g, Wako Pure Chemicals), and an acetylene black powder (0.2 g, Denkikagakukougyo). The current collector was a Mo mesh. The negative electrode was a spiral Al wire (99.99% purity, 2 mm diam.). The reference electrode was an Al wire immersed in the molten AlCl_3 -NaCl saturated with NaCl. It was isolated from the bulk electrolyte with a G4 glass frit at one end.

The assembly of cells and all electrochemical measurements were carried out in a dry N₂ atmosphere. The cells were placed in thermostated furnaces. The charge-discharge cycling test was performed at 30 mA cm⁻² and 170°C. The working electrode for the cyclic voltammetry and the *ac* impedance measurement was a flat FeS plate (0.35 cm², Wako Pure Chemicals). The electrode surface was polished by no. 1200 sandpaper and fine alumina powder (3 μm) followed by degreasing with methanol. The counter was also a spiral Al wire.

The cyclic voltammograms were obtained with a potentiogalvanostat (Nikko Keisoku, NPGS-301S) and function generator (Nikko Keisoku, NFG-5), and a x-y recorder (Watanabe Sokki). The experimental set-up for the *ac* impedance measurements consisted of the Frequency Response Analyzer (FRA: NF Kairo, S-5702B) and the potentiogalvanostat. The real (Re) and imaginary (Im) part of the impedance data were calculated by the FRA which was controlled by a NEC-PC9801E computer. Ten points per decade of impedance measurements were made in the frequency range of 10 kHz-50 mHz.

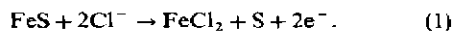
The product formed on the FeS electrode was identified by the X-ray analysis and the scanning electron microscopy (SEM).

RESULTS AND DISCUSSION

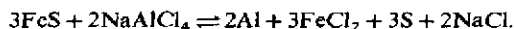
Figure 1 shows the typical charge-discharge curves of the positive electrode for the Al/FeS₂ cell at 170°C and at various cycle numbers. The discharge capacity significantly decreases with increasing cycle number from 200 to 300 cycles. It is noted that the slope of the charging curve remarkably increases from 100 cycles, but the discharging curves have a stable plateau at various cycle numbers. The capacity decline may be caused by the difficulty of deep charge. Such a change in the charging curve was attributed to the charge reaction processes. Then, the charge reaction was studied to improve the rechargeability.

The electrochemical behavior of FeS was investigated by cyclic voltammetry. Figure 2 shows the typical

voltammogram of an FeS electrode in the NaCl saturated AlCl₃-NaCl melt without Al₂S₃ at 200°C. Only an anodic wave appears, and the anodic current flows at about 2.0 V vs Al. This anodic reaction may be the oxidation of FeS to form S and FeCl₂ as in the following reaction:



We calculated the equilibrium potential at 200°C for the reaction:



It was found to be 2.17 V using available thermodynamic data[6, 7]. The observed anodic potential agreed with this calculated value.

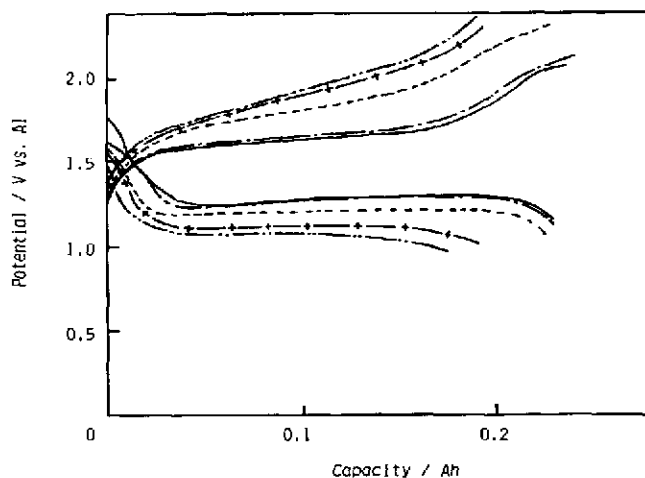


Fig. 1. Typical charge-discharge curves for the FeS₂ electrode at various cycle numbers and 170°C. $I = 30$, —: 10, - - - -: 100, - - - -: 200, - + - +: 250, - · - ·: 300 mA cm⁻².

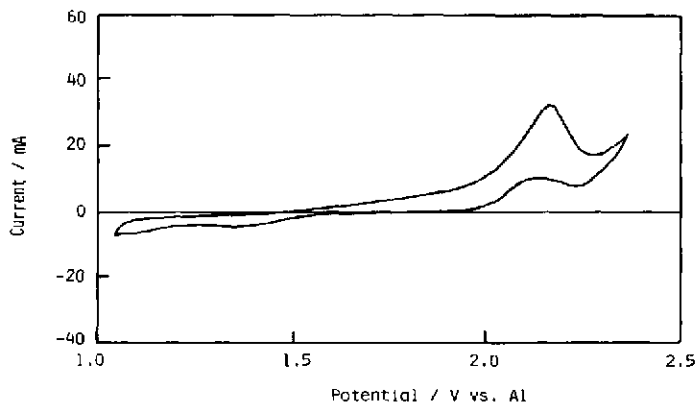


Fig. 2. Cyclic voltammogram of FeS electrode in a NaCl saturated AlCl₃-NaCl at 200°C. Sweep rate: 0.05 v s⁻¹; Electrode area: 0.35 cm².

Cyclic voltammetry of the FeS electrode in the melt with Al_2S_3 was performed. Typical voltammograms for the FeS electrode in the melt with $4 \times 10^{-2} \text{ M Al}_2\text{S}_3$ at various sweep rates are shown in Fig. 3. The left edge for anodic peak and the right edge for cathodic peak appear at 1.40–1.43 V and 1.30–1.34 V, respectively. Figure 4a and b show that the cathodic peak currents (i_{cp}) and potentials (E_{cp}) are proportional to the square root of the sweep rate, which is the expected behavior under ohmic control[8]. This cathodic behavior is the same as that of the positive electrode in the Al/FeS₂ cell[4]. These results were also similar to the cathodic behavior of an Fe electrode in LiCl–KCl melt with Li_2S [9]. The anodic peak currents (i_{ap}) were also proportional to $v^{1/2}$ as shown in Fig. 5, but a large shift with increasing sweep rate was observed for the peak potential of the anodic reaction. Such a large shift may be due to different resistances for the FeS and FeS₂ electrodes.

In order to determine the composition of the deposited material, the FeS electrode was potentiostated at 1.50 V for 24 h in the $6.7 \times 10^{-2} \text{ M Al}_2\text{S}_3$ added melt at 200°C. FeS₂ was significantly detected by X-ray diffraction. Figure 6 shows the morphology of the surface of the deposited FeS electrode. The white parts seem to be FeS₂ particles. From these results, the anodic wave in Fig. 3 indicates the sulfidation from FeS to FeS₂. The anodic sulfidation process was also investigated by *ac* impedance measurements. Figure 7 shows the complex plane plots for the FeS electrode in the $2 \times 10^{-2} \text{ M Al}_2\text{S}_3$ added melt at various controlled potentials at 200°C. The impedance spectra have straight lines with an angle of about 45° in the potential range of 1.40–1.45 V. At 1.50–1.55 V, the spectra became lines with lower angles which bent at low

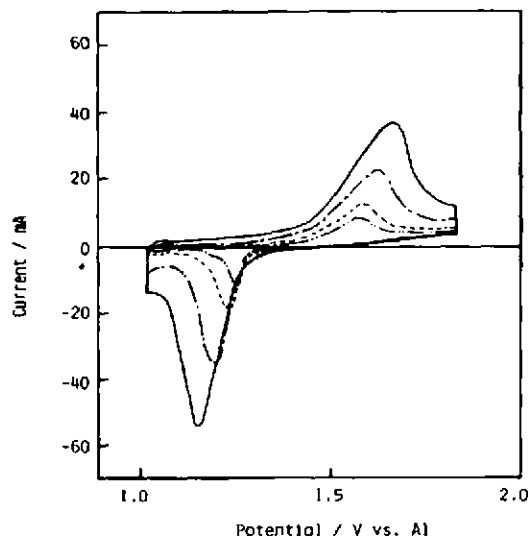


Fig. 3. Cyclic voltammograms of FeS electrode in a NaCl saturated AlCl_3 – NaCl melt with $4 \times 10^{-2} \text{ M Al}_2\text{S}_3$ at various sweep rates and 200°C. Electrode area: 0.35 cm^2 ; —: 0.050 V s^{-1} , — — —: 0.025 V s^{-1} , - - - -: 0.010 V s^{-1} , - · - · -: 0.005 V s^{-1} .

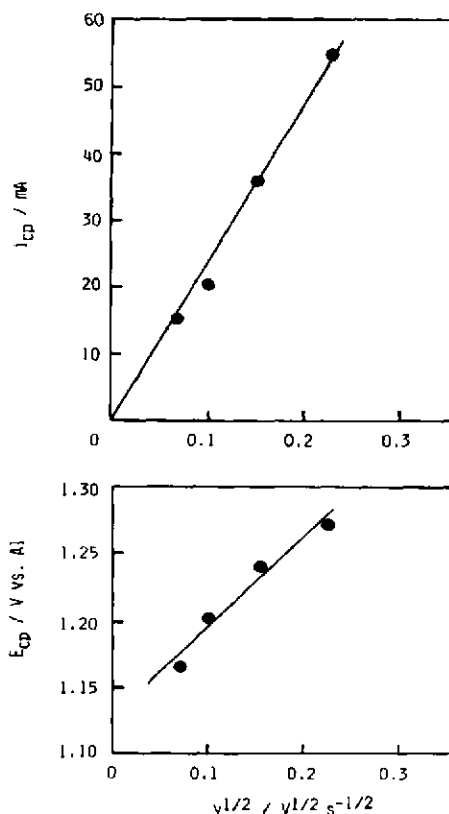


Fig. 4. Relationships between i_{cp} or E_{cp} and $v^{1/2}$.

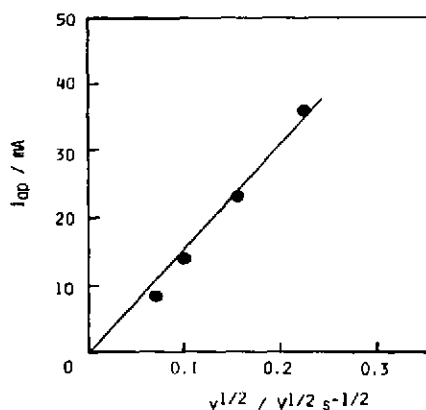


Fig. 5. Relationship between i_{ap} and $v^{1/2}$.

frequencies. This fact may be attributed to an effect of the nucleation process because the rate determining step on extended polarization is generally expected to be the nucleation process.

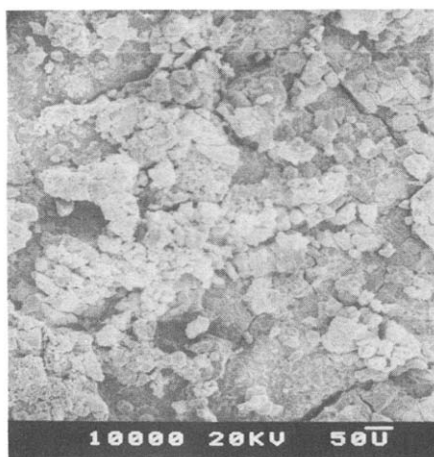


Fig. 6. SEM photograph of the surface of FeS electrode anodized at 1.50 V and 200°C for 24 h.

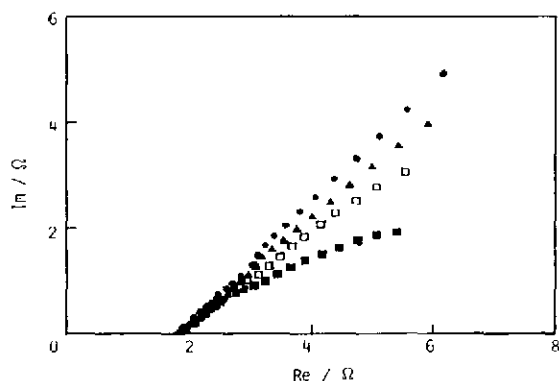


Fig. 7. Complex-plane plots of FeS electrode in AlCl_3 -NaCl melt with 2×10^{-2} M Al_2S_3 at various anodic potentials and 200°C. ●: 1.400 V; ▲: 1.450 V; □: 1.500 V; ■: 1.550 V.

Moreover, we investigated the impedance behavior at a slightly polarized potential (1.450 V) without the nucleation effect. Figure 8 shows typical Randles plots for the FeS electrode in the melt with 2×10^{-2} M Al_2S_3 at 200°C. Two parallel straight lines are seen, which indicate that the current-controlling reaction is the diffusion process. The Warburg slope, σ , can be obtained from the slope of either Re or Im versus $\omega^{-1/2}$. Then σ can be generally expressed by the following equation:

$$\sigma = RT/n^2 F^2 \sqrt{2} A_s \Sigma (1/D_i)^{1/2} C_i \quad (2)$$

where D_i is the diffusion coefficient ($\text{cm}^2 \text{s}^{-1}$), C_i is the bulk concentration of reacting species (mol cm^{-3}), A_s is the electrode area (cm^2), and n is the number of electrons transferred.

In addition, the σ values were obtained in melts containing various Al_2S_3 concentrations. It was assumed that the dissolved Al_2S_3 forms a sulfide ion such

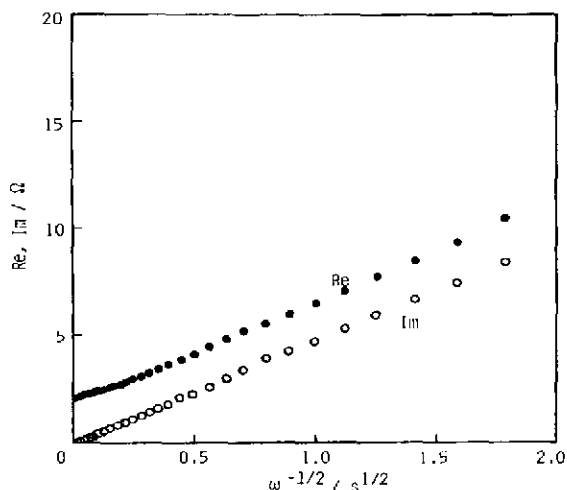
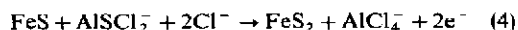


Fig. 8. The Randles plots of FeS electrode in AlCl_3 -NaCl melt with 2.0×10^{-2} M Al_2S_3 at 200°C.

as S^{2-} , and that the concentration of S^{2-} ($C_{\text{S}^{2-}}$) is three times as large as the Al_2S_3 concentration. Figure 9 shows the plots of σ versus $1/C_{\text{S}^{2-}}$. The values of σ are proportional to $1/C_{\text{S}^{2-}}$. This fact agrees with the relationship between σ and $1/C_{\text{S}^{2-}}$ of Equation (2). Moreover, this suggested that the anodic reaction is controlled by diffusion of the sulfide ion. The electrochemistry of sulfur and sulfide ions in AlCl_3 -NaCl melts is highly dependent on the melt composition[10-12]. In the basic melt, NaAlSCl_2 is formed by the dissolution of Al_2S_3 as in the following reaction[13, 14]:



Namely, it is considered that the sulfide ion in the NaCl saturated AlCl_3 -NaCl melt with Al_2S_3 exists mainly as AlSCl_2^- . We propose that the anodic reaction in the basic melt is controlled by diffusion of AlSCl_2^- as in the following reaction:



If the mechanism of the anodic reaction is represented by the reaction of Equation (4) and the process is controlled by the diffusion of AlSCl_2^- , the diffusion coefficient can be calculated. It was found to be $1 \times 10^{-6} \text{ cm}^2 \text{ s}^{-1}$ at 240°C, $3 \times 10^{-7} \text{ cm}^2 \text{ s}^{-1}$ at 200°C, and $1 \times 10^{-7} \text{ cm}^2 \text{ s}^{-1}$ at 170°C from the slope of σ vs $1/C_{\text{S}^{2-}}$ in Fig. 9 and Eq. (2). In other reports, it was known that the diffusion coefficient of Al_2Cl_7^- in the AlCl_3 -NaCl melt at 175°C is 3.2 - $5.5 \times 10^{-6} \text{ cm}^2 \text{ s}^{-1}$ using cyclic voltammetry[15]. Diffusion coefficients of S^{2-} in MgCl_2 -NaCl-KCl and LiF-NaF eutectic melts with Al_2S_3 at 750°C are $2.73 \times 10^{-5} \text{ cm}^2 \text{ s}^{-1}$ and $1.47 \times 10^{-5} \text{ cm}^2 \text{ s}^{-1}$, respectively[16, 17], and that of S^{2-} in a LiCl-KCl melt at 450°C is $5.2 \times 10^{-5} \text{ cm}^2 \text{ s}^{-1}$ [18]. At low temperatures, the value of the diffusion coefficient of AlSCl_2^- is very small, but it becomes comparable in value with that of Al_2Cl_7^- at 240°C. These observed values are also much smaller

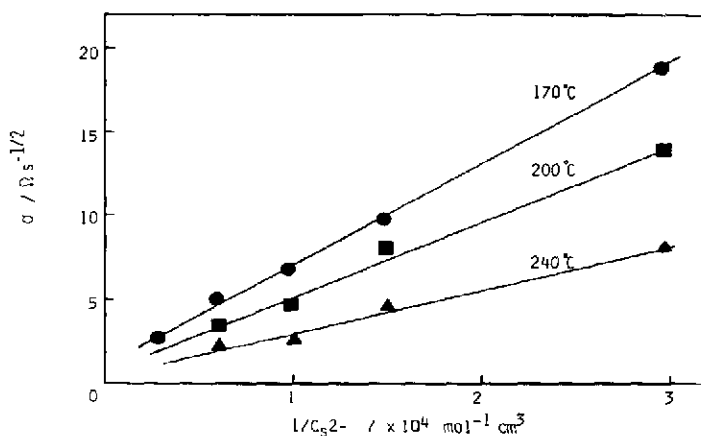


Fig. 9. Plots of σ vs $1/C_{S^{2-}}$ at various temperatures.

than the values of the diffusion coefficient of S^{2-} in other melts. Such variation of the values may be attributed to the increases in the viscosity of the melt or the radius of the diffusing species, because in the basic melts the $AlSCl_2^-$ ion may actually exist as a chain or polymeric species like $(Al_nS_{n-1}Cl_{2n+2})^{n-}$ or $(AlSCl_2)_n^-$, respectively. The value of n would also change significantly with the chloride activity, the sulfide concentration, and the temperature [12, 13].

If the cathodic reaction of the FeS_2 electrode corresponds to the reversed reaction of Equation (4), the Nernst equation for the equilibrium reaction is given by Equation (5).

$$E = E_0 + (RT/2F) \ln [FeS_2][AlCl_4^-] / [FeS][AlSCl_2^-][Cl^-]^2 \quad (5)$$

If it is assumed that the concentrations of FeS_2 , FeS , $AlCl_4^-$, and Cl^- remain constant, then Equation (5) can be simplified to:

$$E = E_0'' - (2.3RT/2F) \log [AlSCl_2^-] \quad (6)$$

It is known from Equation (6) that a slope of $E - \log [AlSCl_2^-]$ is $2.3RT/2F$. The relationship between the sulfide concentration ($C_{S^{2-}}$) and the equilibrium potential of an FeS/FeS_2 electrode couple was studied (Fig. 10). The gradient of the straight line in Fig. 10 is -45 mV. The close agreement of the experimental and theoretical values ($-2.3RT/2F = -45.9$ mV at $190^\circ C$) supports that the equilibrium reaction for FeS and FeS_2 is represented by Equation (4).

CONCLUSIONS

The electrochemical behavior of FeS in molten $AlCl_3-NaCl$ saturated with $NaCl$ containing dissolved Al_2S_3 was studied by cyclic voltammetry, ac impedance measurements, and EMF measurements. Anodic sulfidation of the FeS electrode was characterized as the oxidation reaction from FeS to FeS_2 . This reaction would be controlled by diffusion of the sulfide ion as $AlSCl_2^-$ at a small anodic overpotential.

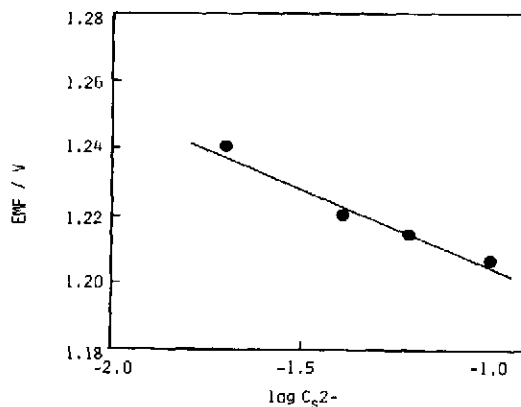
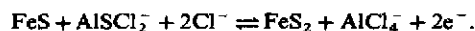


Fig. 10. Relationship between EMF of FeS/FeS_2 electrode couple and $\log C_{S^{2-}}$.

A detailed analysis of the experimental results suggested the following mechanism for the anodic sulfidation of FeS :



The diffusion coefficient of $AlSCl_2^-$ was calculated to be $1 \times 10^{-6} \text{ cm}^2 \text{ s}^{-1}$ at $240^\circ C$.

REFERENCES

1. N. Koura, *J. electrochem. Soc.* **127**, 1529 (1980).
2. N. Koura, T. Inoue and S. Takahashi, *Prog. Batteries Sol. Cells* **3**, 260 (1980).
3. S. Takahashi, N. Koura and T. Inoue, *Nippon Kagaku Kaishi*, **1982**, 1077 (1982).
4. N. Takami and N. Koura, *Denki Kagaku* **54**, 498 (1986).
5. N. Takami and N. Koura, *Electrochim. Acta*, submitted.
6. JANAF Thermochemical Tables, The Bow Chemical Co (1977).

7. L. G. Boxall, H. L. Jones and R. A. Osteryoung, *J. electrochem. Soc.* **120**, 223 (1973).
8. A. J. Calandra, N. R. de Tacconi, R. Pereiro and A. J. Arvia, *Electrochim. Acta* **19**, 901 (1974).
9. C. A. Melendres, C. C. Sy and B. Tani, *J. electrochem. Soc.* **124**, 1060 (1977).
10. R. Marassi, G. Mamantov and J. Q. Chambers, *J. electrochem. Soc.* **123**, 1128 (1976).
11. K. A. Paulsen and R. A. Osteryoung, *J. Am. chem. Soc.* **98**, 6866 (1976).
12. J. Robinson, B. Gilgert and R. A. Osteryoung, *Inorg. Chem.* **169**, 3040 (1977).
13. R. W. Berg, S. V. Winbush and N. J. Bjerrum, *Inorg. Chem.* **19**, 2688 (1980).
14. H. A. Hjuler, R. W. Berg, K. Zachariassen and N. J. Bjerrum, *J. chem. Eng. Data* **30**, 203 (1985).
15. P. Rolland and G. Mamantov, *J. electrochem. Soc.* **123**, 1299 (1976).
16. N. Q. Minch, R. O. Loutfy and N. P. Yao, *J. electroanal. Chem.* **131**, 229 (1982).
17. N. Q. Minch and N. P. Yao, *J. electrochem. Soc.* **130**, 1025 (1983).
18. D. Warin, Z. Tomczuk and D. R. Visser, *J. electrochem. Soc.*, **130**, 64 (1983).